Paper No.
3

CORROSION96
The NACE International Annual Conference and Exposition

ELECTROCHEMICAL PROPERTIES OF IRON DISSOLUTION IN THE PRESENCE OF CO_2 - BASICS REVISITED

Srdjan Nesic, Nicolas Thevenot,
Institutt For Energiteknikk
P.O.Box 40
N-2007 Kjeller - Norway

Jean-Louis Crolet
Elf Aquitaine
64018 Pau - France

Dragutin M. Drazic
Faculty of Technology and Metallurgy
University of Belgrade
P.O.Box 494
11001 Belgrade - Yugoslavia

ABSTRACT

In order to shed more light on the anodic reaction mechanism in CO_2 corrosion of mild steel, two different kinds of electrochemical measurements were used : potentiodynamic sweep and galvanostatic measurements. Experiments were conducted in a glass cell at room temperature (T=22 ± 1 °C), different CO_2 partial pressures (0 - 1 *bar*), over a broad pH range (2-7) using a rotating cylinder at 4000 *rpm*.

Distinct and different anodic mechanisms were observed for pH<4 and for pH>5. In the intermediate area there seems to be a transition from one mechanism to another. New orders of reaction and Tafel slopes were extracted, very different from what was previously assumed. A coherent ensemble of mechanisms was proposed for the anodic reaction which is consistent with the experimental results.

Consequences of the present findings for the CO_2 corrosion area are discussed. For example, in the case of undissolved iron carbide layers, it is no longer possible to discriminate the roles of galvanic coupling and internal acidification.

Keywords : CO_2 corrosion, anodic reaction, mechanism, carbon steel.

INTRODUCTION

CO_2 corrosion of steel as related to oil and gas production and transportation is an area of large practical and economical interest. Consequently a significant body of research has been generated over the past few decades related to various studies of parameters affecting CO_2 corrosion.* However it is difficult to explain that there are very few studies of the basic corrosion mechanisms even for the simplest case of bare steel surfaces corroding in a controlled laboratory environment. Even more so it is difficult to interpret results from the numerous parameter studies when the basic corrosion mechanisms remained obscure.

One of the first proposals for a corrosion mechanism of steel in CO_2 solutions included direct reduction of carbonic acid as the dominant cathodic mechanism (de Waard and Milliams[1]). In recent studies [2] it was found that some of the underlying assumptions in their original model are questionable. The authors[1] assumed a first order dependence for iron dissolution with respect to OH^-, however recently[2, 3] it has been clearly experimentally demonstrated that this is not valid in CO_2 solutions. This actually does not come as a big surprise as in the original paper of Bockris et al.[4] (which was used by de Waard and Milliams[1]) the first order of reaction with respect to OH^- was reported only for pH<4, so that direct extrapolation to higher pH is unreliable. Since the assumed mechanism of the anodic reactions was inadequate, the derivations which led de Waard and Milliams[1] to propose the cathodic reaction mechanism, can also be questioned. Many subsequent studies of CO_2 corrosion mechanisms adopted uncritically the same mechanism for iron dissolution, including some of our own.[5]

Since there are no clear studies which were devoted to a detailed investigation of iron dissolution in CO_2 containing solutions, a new experimental program was initiated on this subject. The experimental results presented below enabled us to propose a new reaction scheme which accounts for the effects of pH and CO_2 partial pressure in a correct way.

EXPERIMENTAL

Equipment

Experiments were conducted at atmospheric pressure in a glass cell. A three electrode set-up (Figure 1) was used in all polarisation experiments: a rotating cylinder electrode was used as the working electrode, a platinum ring served as the counter electrode and an external Ag/AgCl reference electrode was connected to the cell via a Luggin capillary with a porous wooden plug.

Material

The working electrode was made from X65 carbon steel rod machined into a cylinder 10 *mm* in diameter and 10 *mm* long. The exposed area of the specimen was 3.14 cm^2. Chemical composition of the steel is given in Table 1.

* Just as an example: our corrosion research group at IFE, Kjeller, Norway, has a local database with more than 1000 articles covering the CO_2 corrosion related areas.

Procedure

The glass cell was filled with 3 litres of electrolyte: distilled water + 0.2 M $NaClO_4$. This salt was chosen as a supporting electrolyte for its well known inert properties.[6] Gas purging (N_2 or CO_2) was used to deoxygenate and equilibrate the solution. In addition, $HClO_4$ or $NaHCO_3$ were added in order to adjust the pH 2-7 in different experiments.

Immediately before each polarisation experiment the steel electrode surface was polished with 500 and 1000 grit silicon carbide paper, washed with alcohol, dried and immersed into the electrolyte.

Experiments were conducted at room temperature (T=22 ± 1 °C) in order to avoid iron carbonate film formation especially at high pH. All measurements were conducted with the cylinder rotating at 4000 *rpm* so that it can be assumed that the concentration overpotential was negligible meaning that the surface concentrations of species were approximately equal to the bulk concentrations. Experimental conditions are summarised in Table 2.

Electrochemical measurements

Two different kinds of electrochemical measurements were employed in the present study: potentiodynamic sweep and galvanostatic measurements.

Potentiodynamic sweeps at different pH and CO_2 partial pressures were conducted using a scan rate of 1 *mV/s*. During introductory experiments it was determined that this rather fast scan rate did not give significantly different results compared to 0.1 *mV/s* scan rate (Figure 2). After each experiment, an *iR* drop measurement was conducted using the AC impedance technique. In all experiments it was found that the solution resistance was lower than 0.5 Ω corresponding to a correction of 10 *mV* at the current density of 10 mA/cm^2. From these sweeps it is possible to extract both the order of reaction (with respect to OH^- and CO_2) and a Tafel slope for the anodic reaction (Figures 3 - 8).

Galvanostatic measurements were conducted by applying a constant anodic current (1 mA/cm^2) and measuring the potential for different pH and CO_2 partial pressures. If a general expression for the anodic current is considered :

$$i_a = k\left[OH^-\right]^{a_1}\left[p_{CO_2}\right]^{a_2} \exp\left(\frac{\alpha_a F}{RT} E\right) \qquad (1)$$

where:

$[OH^-]$	is the hydroxide ion concentration, M;
p_{CO_2}	partial pressure of CO_2 , *bar*;
a_1, a_2	respective orders of reaction;
α_a	apparent transfer coefficient;
F	Faraday constant (96490 *C/equiv.*);
R	universal gas constant (8.3143 *J/(mol K)*);
T	absolute temperature, *K*;
E	overpotential, *V*.

At a constant current density and CO_2 partial pressure the potential as a function of pH can be expressed as:

$$E = -a_1 \cdot b_a \cdot pH + \text{constant} \tag{2}$$

where $b_a = 2.303RT/\alpha_a F$ is the anodic Tafel slope in V per decade.

Thus from a plot of "E vs. pH" the measured slope of the curve $a_1 \cdot b_a$ is the product: [order of reaction]×[anodic Tafel slope] so that with these measurements it was possible to double-check the results obtained from the potentiodynamic sweeps. In a similar fashion for a constant pH under galvanostatic conditions the potential E can be expressed as a function of p_{CO_2}:

$$E = -a_2 \cdot b_a \cdot \log(p_{CO_2}) + \text{constant} \tag{3}$$

Comment. It should be mentioned that, in order to complete the study, electrochemical measurements (potentiodynamic sweeps, corrosion potential and polarisation resistance measurements) were also used to investigate the mechanism of the cathodic reactions. However, it was not easy to draw any firm conclusions since the limiting currents were reached for small overpotentials and no clear Tafel region could be identified.

EXPERIMENTAL RESULTS

In order to facilitate interpretation of the results they are separated into three groups. Distinct and different mechanisms were observed for pH<4 and for pH>5. In the intermediate area there seems to be a transition from one mechanism to another.

The effect of pH and CO_2 partial pressure are described separately in the next paragraphs. Such a treatment is possible since both dissolved CO_2 and carbonic acid concentrations are independent from pH and proportional to p_{CO_2}.

Potentiodynamic sweeps

pH effect

- **pH<4**. In CO_2 solutions very different anodic Tafel slopes and orders of reaction were obtained from what was expected from the mechanism proposed by Bockris et al.[4] (in further text denoted as the BDD mechanism). This is true when analysing the potentiodynamic anodic sweeps both at 0.2 *bar* (Figure 3) and at 1 *bar* (Figure 4) . In the presence of CO_2 at low pH the Tafel slopes were observed varying from 20 to 35 *mV* per decade. The order of reaction with respect to the pH was no doubt larger than 1 with the majority of the values oscillating around 2.
- **4<pH<5**. Potentiodynamic sweeps in this intermediate pH range which is very common in CO_2 corrosion studies were also the most difficult to interpret (Figure 5, 6). Tafel slopes varying from 30 to 60 *mV* per decade were observed and the order of reaction with respect to pH changing from 2 to 1

and going toward 0 as pH was increasing. This suggests that 4<pH<5 is a transition region leading from one anodic mechanism to another.

- **pH>5**. Similar as previously reported [2,3] in the present study it was found that the influence of the pH on the dissolution rate of iron completely vanished for pH>5 (Figure 7, Figure 8). Anodic Tafel slopes as high as 80 to 120 mV per decade were clearly observed.

CO_2 effect. If we compare the potentiodynamic sweeps conducted at pH 2.5 but at two different CO_2 partial pressures: p_{CO_2} = 0.2 and 1 *bar* (Figure 9) the anodic line is shifted by a factor of two. The same was found at pH 6 (Figure 10). This suggests for this p_{CO_2} range an order of reaction with respect to CO_2 of 0.4. The same behaviour was observed over the whole range of pH studied (2.5 - 6).

All previous results obtained from the polarisation sweeps were double checked with galvanostatic measurements presented below.

Galvanostatic measurements

In these measurements the applied anodic current was chosen high enough so that the cathodic partial current would be negligible, but again low enough to avoid any passivation. After considering the potentiodynamic sweep data and some trial and error, the final galvanostatic experiments were conducted at a current of 1 mA/cm^2 (3.14 mA).

pH effect

- **pH<4**. From Figure 11 a slope of about 60 mV per pH unit was found for the CO_2 purged solution. Considering the previously discussed potentiodynamic sweep results by using (2) this slope can be interpreted as the product of the order of reaction of 2 and the 30 mV per decade Tafel slope. For the N_2 purged solution a slope of 40 mV per pH unit was measured, which agrees well with the BDD mechanism [4] (product of an order of reaction of 1 with a 40 mV per decade Tafel slope). Obviously the mechanism for iron dissolution in CO_2 solutions is different from the one obtained in strong acids.
- **4<pH<5**. It was difficult to interpret the galvanostatic data in this region (Figure 11) where the slope of the line changes from 60 mV per pH unit to zero. It can only be confirmed that this is a transition region between the two mechanisms for iron dissolution.
- **pH>5**. In this region the measured potential did not change with pH, confirming a zero order of reaction with respect to OH^- found with the potentiodynamic sweeps. However, it is impossible to extract any information about the Tafel slope for this region.

CO_2 effect. In order to study the CO_2 effect, galvanostatic measurements at 1 mA/cm^2 were conducted at pH 3.6 (constant), while p_{CO_2} was gradually increased from 0 to 1 *bar*. As expected from the potentiodynamic sweeps (Figures 9 and 10) a decrease in the potential with increasing p_{CO_2} was observed (Figure 12). The effect of p_{CO_2} becomes noticeable for p_{CO_2} >0.1 *bar* and seems to vanish after p_{CO_2} >1 *bar*. When the transient region of the curve in Figure 12 is fitted with a straight line as a first

approximation, a slope of 30 mV per decade is obtained. If we recall that at this pH a Tafel slope of 30 mV per decade was measured (Figure 3 and 4) with the help of equation (3) an order of reaction with respect to CO_2 of 1 is obtained. It should be noted that as $p_{CO_2}=1\ bar$ is approached the order of reaction is reduced what agrees with the previous observation that between 0.2 and 1 bar the order of reaction is approximately 0.4. As a double-check, from Figure 12 a decrease of about 10 mV occurs between 0.2 and 1 bar what agrees with the value extracted from the potentiodynamic sweeps (Figure 9).

Experimental results - summary

From all previously shown experiments it is possible to derive the general experimental form of the iron dissolution rate equation*:

$$i_a = k\left[OH^-\right]^{a_1}\left(p_{CO_2}\right)^{a_2} 10^{\frac{E}{b_a}} \qquad (4)$$

where for:

pH<4	$\Rightarrow$	a_1=2	; b_a=0.03 V per decade¤
4<pH<5	$\Rightarrow$	a_1=2÷0	; b_a=0.03→0.12 V per decade
pH>5	$\Rightarrow$	a_1=0	; b_a=0.12 V per decade
$p_{CO_2}<10^{-2}\ bar$	$\Rightarrow$	a_2=0	
$10^{-2}<p_{CO_2}<1\ bar$	$\Rightarrow$	a_2=1	
$p_{CO_2}>1\ bar$	$\Rightarrow$	a_2=0	

DISCUSSION

Proposal of anodic mechanisms

In the following discussion we have selected only the mechanisms (among the many we considered) which were in best agreement with the experimental findings. In the analysis it will be assumed that the order of reaction with respect to CO_2 is 1, keeping in mind that this order vanishes when $0.01\ bar > p_{CO_2} > 1\ bar$ what will be discussed later.

pH<4. Let us recall the experimental rate equation for the anodic reaction in this pH range:

---

* This study was focused on revealing the mechanisms so accordingly the rate constants in all reactions were denoted with a generic k.

¤ The Tafel slope $b_a = 2.303RT/\alpha_a F$ is shown for room temperature (22°C).

$$i_a = k\left[OH^-\right]^2 p_{CO_2} \exp\left(\frac{2FE}{RT}\right) \quad (4)$$

In order to explain the different kinetics of iron dissolution in CO_2 solutions compared to strong acids, it is proposed to consider a carbonic species as a chemical ligand catalysing the dissolution of iron. H_2CO_3 and dissolved CO_2 are the only ones whose concentrations do not depend on pH, and since the concentration of CO_2 is far higher, let us assume that :

$$Fe + CO_2 \Leftrightarrow Fe_L \quad (5a)$$

Fe_L stands for the ligand, an intermediate in the following mechanism.

Such preliminary step is in agreement with the experimental observation that the p_{CO_2} influence did not change with pH. Consequently the following mechanism can be proposed to explain the experimental results:

$$Fe_L + H_2O \Leftrightarrow Fe_LOH_{ad} + H^+ + e^- \quad (5b)$$

$$Fe_LOH_{ad} \Leftrightarrow Fe_LOH^+_{ad} + e^- \quad (5c)$$

$$Fe_LOH^+_{ad} + H_2O \Leftrightarrow Fe_L(OH)_{2\,ad} + H^+ \quad (5d)$$

$$Fe_L(OH)_{2\,ad} \xrightarrow{rds} Fe_L(OH)_{2\,sol} \quad (5e)$$

$$Fe_L(OH)_{2\,sol} + 2H^+ \Leftrightarrow Fe^{2+} + CO_2 + 2H_2O \quad (5f)$$

From equation (5a) the first order effect of p_{CO_2} on the iron dissolution rate is obvious. The following steps (5b) to (5f) are equivalent to the mechanism previously proposed by Drazic[7] keeping in mind that :

$$Fe_L = FeCO_{2\,ad} \quad (6)$$

$$Fe_LOH_{ad} = FeHCO_{3\,ad} \quad (7)$$

$$Fe_LOH^+_{ad} = FeHCO^+_{3\,ad} \quad (8)$$

$$Fe_L(OH)_{2\,ad} = FeOH_2CO_{3\,ad} \quad (9)$$

In this mechanism the adsorption of CO_2 an its derivatives plays a similar (intermediary) role as the OH^- has in the BDD mechanism. In addition in CO_2 corrosion, the anodic and cathodic reactions might share the common active adsorbate, as it is observed in nitric acid.[8]

Assuming a low coverage with OH^- (which is a reasonable assumption at this pH), a Langmuir type adsorption isotherm can be used and a dissolution rate can be derived which agrees with the experimental equation (4) . This lengthy derivation is a textbook case [9] and has been shown in the Appendix only once as an illustration.

4<pH< 5. As described in the experimental section, data obtained in this pH region were difficult to interpret. However, it was clear that with an increase in pH the anodic Tafel slope increased while the order of reaction with respect to pH changed from 2 towards zero.

We have here arbitrarily divided the pH region into 3 parts with different mechanisms occurring in the pH<4 and pH>5 regions. In reality there are of course no sharp changes at pH 4 or pH 5 but rather there is continuous transition that leads from one mechanism to another. Here we will actually start with the previously proposed anodic mechanism for pH<4 (equation 5) and try to show how it evolves into a different mechanism at pH>5.

With increasing pH the concentration of OH^- ions increases. As a consequence we can assume that two changes occur:

- *Change of the rds from (5e) to (5c) with increasing pH*

At pH<4, the desorption step (5e) was the rate determining step (rds). As pH increases toward 5, step (5e) might accelerate faster than the charge transfer step (5c) which eventually becomes the new rds (similar is assumed by Drazic et al.[7]). It is assumed that this change takes place before pH 5 and most likely closer to pH 4. We are still assuming a low coverage of the electrode with the OH^-. The new mechanism becomes :

$$Fe + CO_2 \Leftrightarrow Fe_L \tag{10a}$$

$$Fe_L + H_2O \Leftrightarrow Fe_L OH_{ad} + H^+ + e^- \tag{10b}$$

$$Fe_L OH_{ad} \xrightarrow{rds} Fe_L OH^+_{ad} + e^- \tag{10c}$$

$$Fe_L OH^+_{ad} + H_2O \Leftrightarrow Fe_L(OH)_{2\,ad} + H^+ \tag{10d}$$

$$Fe_L(OH)_{2\,ad} \Leftrightarrow Fe_L(OH)_{2\,sol} \tag{10e}$$

$$Fe_L(OH)_{2\,sol} + 2H^+ \Leftrightarrow Fe^{2+} + CO_2 + 2H_2O \tag{10f}$$

Performing the same derivations as for the previous mechanism (see Appendix) a new equation is obtained for the anodic reaction rate in this pH range:

$$i_a = k\left[OH^-\right] p_{CO_2} \exp\left(\frac{3FE}{2RT}\right) \tag{11}$$

This corresponds to an anodic Tafel slope of 40 mV per decade and an order of reaction of 1 with respect to OH^-. Many experimental CO_2 corrosion studies were performed in this pH region [10] and reported similar parameters for the anodic reaction. Since the same result can be predicted from the BDD mechanism [4] this has led numerous researchers to assume that the latter mechanism is valid for their conditions. As it is shown in the present study other mechanisms are possible and actually even more probable.

- *Change of surface coverage with* OH^- *from low to intermediate as pH increases*

With further increase of the pH, the coverage of the surface with OH^- increases and the Langmuir-type adsorption isotherm is no longer valid. It is likely that in this pH range we have an "intermediate" coverage, so that a Frumkin-type isotherm is a more realistic description of the state of the surface. Derivations involving this isotherm are rather lengthy and complex[11] so they will not be shown here. Nevertheless it is not difficult to anticipate that such an isotherm would lead to a decreased order of reaction with respect to the OH^- and a steeper Tafel slope, what was observed in the present experiments.

pH>5. Recall the experimental rate equation for the anodic reaction in this pH range:

$$i_a = k\, p_{CO_2} \exp\left(\frac{FE}{2RT}\right) \tag{4}$$

If we continue with the same line of reasoning as for the lower and intermediate pH range, we can assume that for some high enough pH the surface coverage will become "saturated", meaning that the changes in the bulk concentration of OH^- will not cause any significant change in the surface coverage. Such an assumption is supported in the present experiments by the vanishing of the pH effect iron dissolution for pH>5. In addition this assumption leads to a 120 mV per decade anodic Tafel slope as demonstrated below, which was also observed in our experiments.

We can assume that the mechanism shown for the intermediate pH range (10) is still valid in this pH range. However, for step (10b) we can assume a constant (high) coverage with OH^- for a given partial pressure, which leads to:

$$\left[Fe_L OH_{ad}\right] \approx const \times p_{CO_2} \tag{12}$$

Then it is easy to calculate the anodic reaction rate from the following rds step (10c) :

$$i_a = k\left[Fe_L OH_{ad}\right]\exp\left(\frac{1}{2}\frac{FE}{RT}\right) \tag{13}$$

or finally

$$i_a = k\, p_{CO_2} \exp\left(\frac{1}{2}\frac{FE}{RT}\right) \tag{14}$$

what is in agreement with the experimental observations.

CO_2 effect. In a similar way the coverage of the metal surface with the carbonate species changes with p_{CO_2}. From Figure 12 we can conclude that for p_{CO_2} <0.01 bar the coverage is insignificant, for 0.01 $bar < p_{CO_2} < 1$ bar there is a Langmuir type dependence while at p_{CO_2} >1 bar "saturation" coverage with the carbonic species is achieved.

Consequences

From the results presented so far it is clear that the previously existing assumption about the mechanism of iron dissolution in CO_2 containing solutions is invalid. The BDD mechanism [4] found in strong acids and pH<4 is not applicable for the case of steel corroding in CO_2 solutions. The fact that for 4<pH<5 in CO_2 solutions there is an anodic Tafel slope of 40 mV per decade and an order of reaction of 1 with respect to pH (what agrees with the BDD mechanism [4]) led to numerous erroneous interpretations. Two such cases are discussed below.

Case #1: Deduction of a cathodic reaction mechanism from corrosion measurements. The explanation of CO_2 corrosion mechanisms presented by de Waard and Milliams [1] is still the most widely referenced and it is instructive to shortly discuss the effect of the present findings on their conclusions. In that study, in order to determine the mechanism of the cathodic reaction, the authors measured the corrosion rate at different pH. Then by assuming the BDD mechanism [4] for the anodic reaction they were able to propose a new mechanism for the cathodic reaction involving direct reduction of carbonic acid. Now, since we know that the BDD mechanism [4] is not correct for this case it would mean that revaluation of the de Waard and Milliams [1] interpretation is needed.

The authors proposed that there should be the following relationship between the corrosion current, pH and p_{CO_2}:

$$\log i_c = -A \cdot pH + B = \tfrac{1}{2} A \cdot p_{CO_2} + B' \tag{15}$$

and determined experimentally the constant to be $A \approx 1.3$. Assuming that the main cathodic reaction is carbonic acid reduction they derived this constant as:

$$A = \frac{2b_k - b_a}{b_k + b_a} \tag{16}$$

Accepting their value for the cathodic Tafel slope b_k=120 mV per decade and by inserting the anodic Tafel slopes for the anodic reaction b_a obtained in the present study (rather than the one from the BDD mechanism [4]) it is found that the constant A is:

$$A = \begin{cases} 1.6 - 1.4 & \text{for } pH < 4 \\ 1.4 - 1.0 & \text{for } 4 < pH < 5 \\ 1.0 - 0.5 & \text{for } pH > 5 \end{cases} \tag{17}$$

It follows that the agreement between the theory of de Waard and Milliams [1] and their own experiments seems to be good only for 4<pH<5 so that the proposed mechanism of the cathodic reactions could be strictly valid only in this range. It is likely that for pH>5 there is a different mechanism or at least a different rate determining step than the one proposed by de Waard and Milliams.[1] Further analysis of the cathodic reaction mechanisms extends beyond the scope of the present study and will be addressed in the near future.

Case #2: Effect of undissolved iron carbide layer on CO_2 corrosion of mild steel. Iron carbide (cementite, Fe_3C) films are often labelled as the "uncorroded portion of the metal". Surface films consisting predominantly of iron carbide are often present when ferritic/perlitic steels with sufficient carbon content corrode in CO_2 containing environment. Such films are very porous and often non-protective. It has been found that such films in some cases can even increase the corrosion rate.[10] It has been originally assumed that this phenomenon occurs via a galvanic effect [12] (where iron carbide film acts as a large cathode). Recently this interpretation was discarded in favour of an alternative explanation based on the concept of internal acidizing under a non-protective film.[5] For the latter explanation, the available knowledge of the kinetics of iron dissolution was extensively used (BDD mechanism [4]). The present, more accurate, knowledge of the anodic kinetics calls for a revaluation of the latter explanation.

In order to distinguish between the two explanations (galvanic coupling vs. internal acidification) pseudo-polarisation plots were used.[5] These are plots of the time development of the corrosion current vs. the corrosion potential (trajectory of the corrosion point). In case of CO_2 corrosion with carbide film development measurements have shown that both the corrosion current and potential increase leading to the slope of the pseudo-polarisation curve of 120 mV per decade. Since the galvanic effect is based on the assumption of an increasing cathode this would lead to a slope of the pseudo-polarisation curve equal to the anodic Tafel slope. Previously it was assumed that the Tafel slope of the anodic line is 40 mV per decade (from the BDD mechanism [4]) so that the galvanic coupling explanation was discarded as impossible. In the light of the present findings this line of reasoning is no longer feasible:

- For pH>5 the anodic Tafel slope of approximately 120 mV per decade and a zero order of reaction with respect to pH were found in the present study. Then any variation of the cathodic curve will yield the same slope of the pseudo-polarisation line (120 mV per decade), whether it comes from the variation of the local pH or the galvanic coupling (Figure 13).
- For pH<4 the anodic Tafel slope of approximately 30 mV per decade and a 2 order of reaction with respect to OH^- were found in the present study. Then the rederivation of the previous calculation[5] for internal acidizing leads to a slope of 180 mV per decade. However, any combination of this effect with galvanic coupling will decrease this slope significantly (Figure 14). This means that the experimentally observed slopes of the pseudo-polarisation lines cannot be explained by one or the other effect alone, but rather with a combination of both.

CONCLUSIONS

Distinct but different anodic mechanisms for iron dissolution in CO_2 solutions were observed for pH<4 and for pH>5. In the intermediate area there seems to be a transition from one mechanism to another. From the potentiodynamic and galvanostatic experiments it was possible to derive the general experimental form of the iron dissolution rate equation for the two distinct pH regions.

A coherent ensemble of mechanisms was proposed for the anodic reactions which are consistent with the experimental results. These are compactly shown in Table 3 . In derivation of these mechanisms special care was needed to describe the electrode coverage with the anions.

Any future analysis or modelling of the CO_2 corrosion mechanisms has to account for the newly discovered kinetics of iron dissolution. Even if the present interpretation of the mechanisms is found to be in error and can be replaced with better proposals, the experimental findings on the orders of reactions and Tafel slopes are a firm basis for future progress in understanding of the CO_2 corrosion phenomena.

One of the first consequences of the present findings is the reinterpretation of the effect of porous iron carbide films often found in corrosion of carbon steels in CO_2 environments. The observed lack of protectiveness of such films can be attributed to a combined effect of galvanic coupling and/or internal acidizing.

REFERENCES

1. C. de Waard and D. E. Milliams, Corrosion, 31 (1975):p.131.

2. S. Nesic, J. Postlethwaite, S. Olsen, "An electrochemical model for prediction of CO_2 corrosion", CORROSION/95, paper no. 131, (Houston, TX: NACE International, 1995).

3. K. Videm, Progress in the Understanding and Prevention of Corrosion, Proceedings from 10th European Corrosion Congress, (London, Institute of Metals, 1993), vol. 1, p.513.

4. J. O .M. Bockris, D. Drazic and A. R. Despic, "The Electrode Kinetics of the Deposition and Dissolution of Iron", Electrochimica Acta, vol.4(1961): p.325.

5. J. L. Crolet, S. Olsen and W. Wilhelmsen, "Influence of a Layer of Undissolved Cementite on the Rate of CO_2 Corrosion of Carbon Steel", CORROSION/94, paper no. 4, (Houston, TX: NACE International, 1994).

6. D. M. Drazic, "Iron and its Electrochemistry in an Active state", Modern Aspects of Electrochemistry, (Plenum Press, 1989), vol. 19, p.79.

7. D. M. Drazic, C. Shen Hao, "Anodic processes on an iron electrode in neutral electrolytes", Bulletin de la Société Chimique Beograd, 47, 11(1982): pp 649-659.

8. C. Gabrielli, M. Keddam, E. Stupnisek-Lisac, H. Takenouti, Electrochimica Acta, 21, 10(1976): p. 757.

9. J. O'M. Bockris, A. K. N. Reddy, Modern Electrochemistry, (New-York, Plenum Press 1973): p.1083.

10. A. Dugstad, L. Lunde, K. Videm, "Parametric study of CO_2 corrosion of carbon steel", CORROSION/94, paper no. 14, (Houston, TX: NACE International, 1994) .

11. E. Gileadi, Electrode Kinetics, (New York, VCH Publishers 1993): p.275.

12. R. Jasinski, "Corrosion of N80 Type Steel by CO_2/Water Mixtures", Corrosion, 43, 4(1987): p. 214.

TABLES

Table 1. Chemical composition of the carbon steel X65 used for the working electrode (mass%).

C	Mn	Si	P	S	Cr	Cu	Ni	Mo	Al	V	Sn	Ti	Nb
0.065	1.54	0.25	0.013	0.001	0.05	0.04	0.04	0.07	0.041	0.035	0.002	0.002	0.041

Table 2. Experimental conditions.

Test solution	$NaClO_4$: 0.2M
Test material	low carbon steel: X65
Pressure	1 and 0.2 *bar* CO_2 and other mixtures, 1 *bar* N_2
Velocity	4000 *rpm*
pH	2-7
Sweep rate	1 *mV/s*
Potentiodynamic sweep limits	0 mV - +150 mV vs. E_{oc}
AC impedance	+/- 5 mV vs. E_{oc} from 500 Hz to 5 kHz
IR compensation T = 20°C	R < 0.5 Ohm
Polarisation resistance	From -5 to +5 mV vs. E_{oc}
Sample area	3.14 cm^2

Table 3. A coherent ensemble of mechanisms for the anodic reactions which are consistent with the experimental results

pH	ANODIC REACTION
Low pH<4	**(A-1)** Low coverage with OH^- and CO_2 (1) $Fe + CO_2 \Leftrightarrow Fe_L$ (2) $Fe_L + H_2O \Leftrightarrow Fe_L OH_{ad} + H^+ + e^-$ (3) $Fe_L OH_{ad} \Leftrightarrow Fe_L OH^+_{ad} + e^-$ (4) $Fe_L OH^+_{ad} + H_2O \Leftrightarrow Fe_L(OH)_{2\,ad}$ (5) $Fe_L(OH)_{2\,ad} \xrightarrow{rds} Fe_L(OH)_{2\,sol}$ (6) $Fe_L(OH)_{2\,sol} + 2H^+ \Leftrightarrow Fe^{2+} + H_2CO_3$ $\boxed{i_a = k\left[OH^-\right]^2 p_{CO_2} \exp\left(2\frac{FE}{RT}\right)}$
Intermediate 4<pH<5	**(A-2)** Same mechanism as **(A-3)** assuming low coverage with OH^- and CO_2 $\boxed{i_a = k\left[OH^-\right] p_{CO_2} \exp\left(\frac{3}{2}\frac{FE}{RT}\right)}$
High pH>5	**(A-3)** High coverage with OH^- and low coverage with CO_2 (1) $Fe + CO_2 \Leftrightarrow Fe_L$ (2) $Fe_L + H_2O \Leftrightarrow Fe_L OH_{ad} + H^+ + e^-$ (3) $Fe_L OH_{ad} \xrightarrow{rds} Fe_L OH^+_{ad} + e^-$ (4) $Fe_L OH^+_{ad} + H_2O \Leftrightarrow Fe_L(OH)_{2\,ad} + H^+$ (5) $Fe_L(OH)_{2\,ad} \Leftrightarrow Fe_L(OH)_{2\,sol}$ (5) $Fe_L(OH)_{2\,sol} + 2H^+ \Leftrightarrow Fe^{2+} + H_2CO_3$ $\boxed{i_a = k\, p_{CO_2} \exp\left(\frac{1}{2}\frac{FE}{RT}\right)}$

APPENDIX

From the proposed mechanism (17) a theoretical expression for the rate of iron dissolution is derived below. The first step (5a) is in chemical equilibrium and if we assume that the adsorption of the carbonic species on the surface is far from saturation, it can be written :

$$Fe_L = k\left[H_2CO_3\right] = k\,p_{CO_2} \tag{A1}$$

The second step (5b) is a charge transfer step involving adsorption. Since it also is in equilibrium we can write :

$$k\,p_{CO_2}\left[OH^-\right](1-\theta_T)\exp\left(\frac{1}{2}\frac{FE}{RT}\right) = k\left[Fe_LOH_{ad}\right]\exp\left(-\frac{1}{2}\frac{FE}{RT}\right) \tag{A2}$$

θ_T being the total surface coverage with OH^- intermediates. At low coverage, $1-\theta_T \approx 1$ so equation (A2) can be rewritten as :

$$\left[Fe_LOH_{ad}\right] = k\left[OH^-\right]p_{CO_2}\exp\left(\frac{FE}{RT}\right) \tag{A3}$$

For the second charge transfer step (5c) in equilibrium, it can be written :

$$k\left[Fe_LOH_{ad}\right]\exp\left(\frac{1}{2}\frac{FE}{RT}\right) = k\left[Fe_LOH^+_{ad}\right]\exp\left(-\frac{1}{2}\frac{FE}{RT}\right) \tag{A4}$$

or

$$\left[Fe_LOH^+_{ad}\right] = k\left[Fe_LOH_{ad}\right]\exp\left(\frac{FE}{RT}\right) \tag{A5}$$

If we now substitute $\left[Fe_LOH_{ad}\right]$ from equation (A3) into (A5) we get:

$$\left[Fe_LOH^+_{ad}\right] = k\left[OH^-\right]p_{CO_2}\exp\left(2\frac{FE}{RT}\right) \tag{A6}$$

Finally the desorption rate-determining-step (rds) (5e) gives us the anodic reaction rate equation:

$$i_a = k\left[Fe_L(OH)_{2ad}\right] \tag{A7}$$

According to step (5d) (chemical equilibrium), $\left[Fe_L(OH)_{2ad}\right] = k\left[Fe_LOH^+_{ad}\right]\left[OH^-\right]$

which leads to :

$$i_a = k\left[Fe_LOH^+_{ad}\right]\left[OH^-\right] \tag{A8}$$

Substituting $\left[Fe_LOH^+_{ad}\right]$ from (A6) into (A8) gives us the final form of the anodic rate equation:

$$i_a = k\left[OH^-\right]^2 p_{CO_2}\exp\left(2\frac{FE}{RT}\right) \tag{A9}$$

which fits the experimental equation (4) both for the Tafel slope and order of reaction.

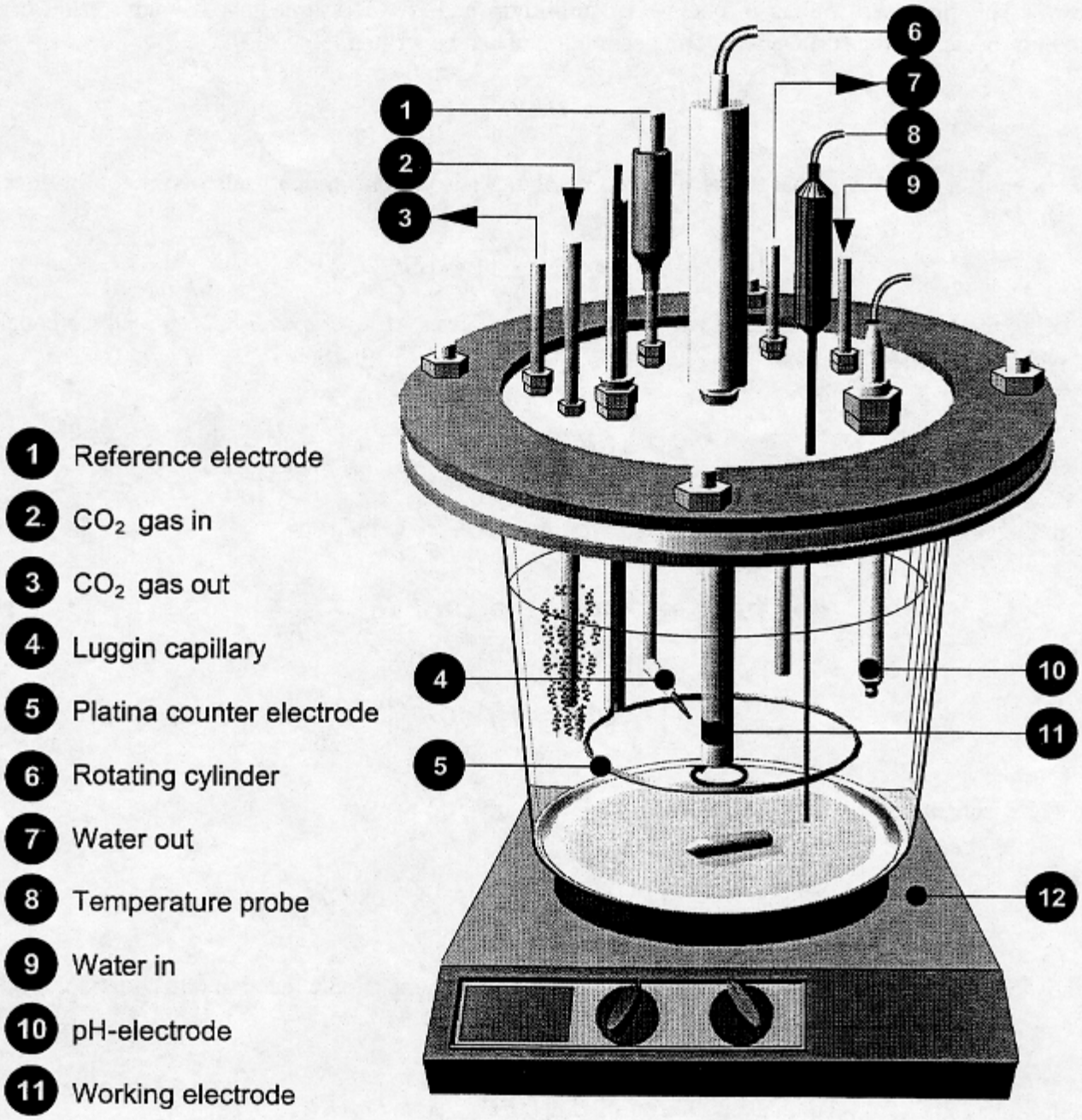

FIGURE 1 - Schematic of the experimental cell

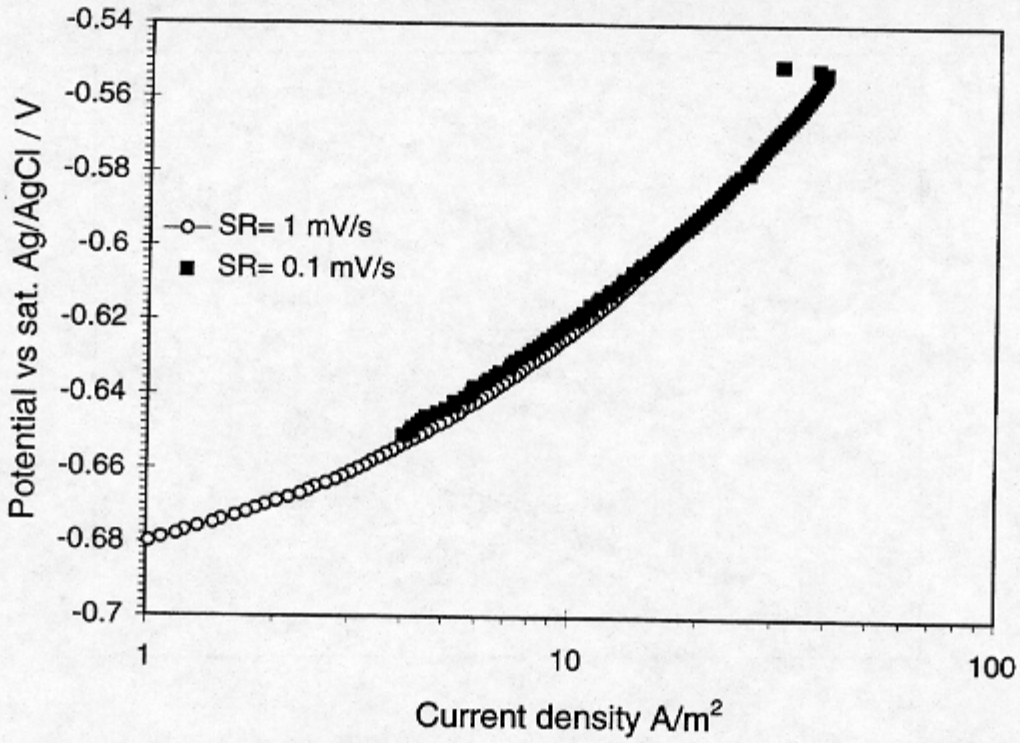

Figure 2 - Potentiodynamic sweeps at two different sweep rates, 1 mV/s and 0.1 mV/s, Pco_2 = 1 *bar*, NaCl = 1%, static conditions, Steel St52.

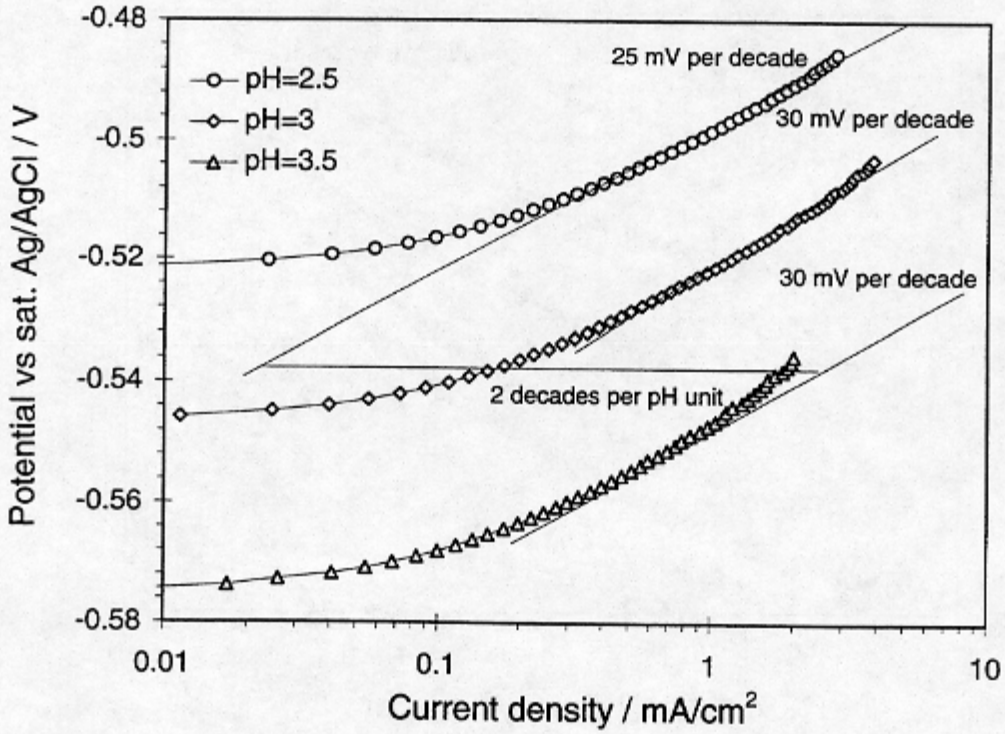

Figure 3 - Potentiodynamic sweeps at low pH and Pco_2 = 0.2 *bar*, sweep rate : 1mV/s, $NaClO_4$: 0.2M, 4000 *rpm*, T = 22C, Steel X65.

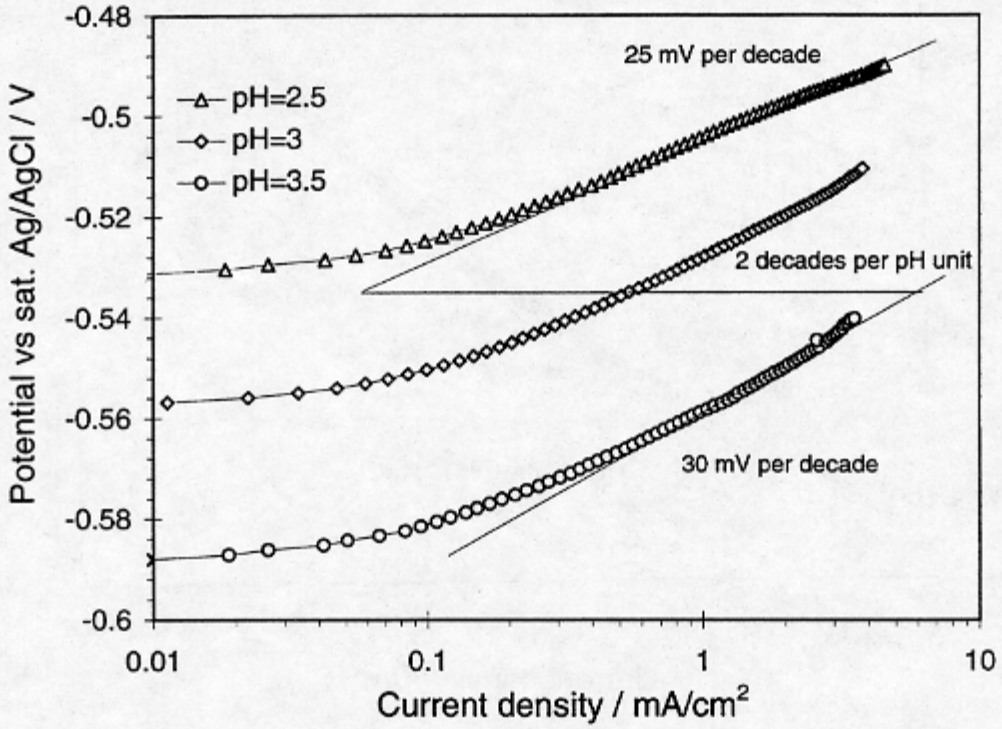

Figure 4 - Potentiodynamic sweeps at low pH and Pco_2 = 1 *bar*, sweep rate : 1 mV/s, $NaClO_4$: 0.2M, 4000 rpm, T = 22C, Steel X65.

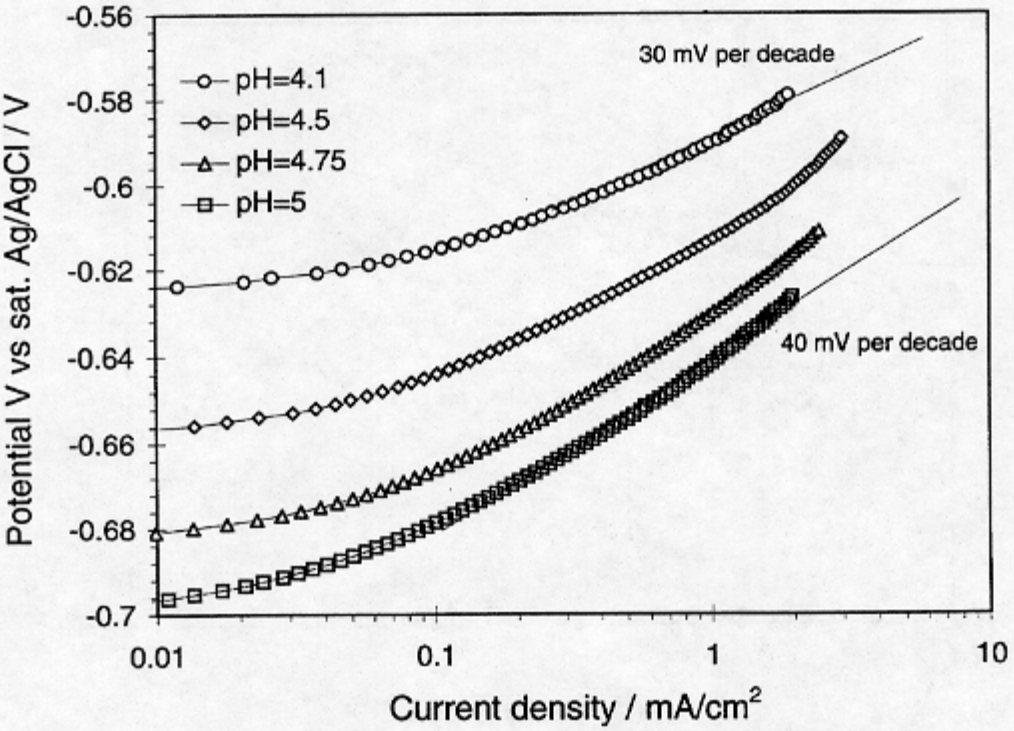

Figure 5 - Potentiodynamic sweeps at intermediate pH and Pco_2 = 0.2 *bar*, sweep rate : 1mV/s, $NaClO_4$: 0.2 M, 4000 rpm, T = 22C, Steel X65.

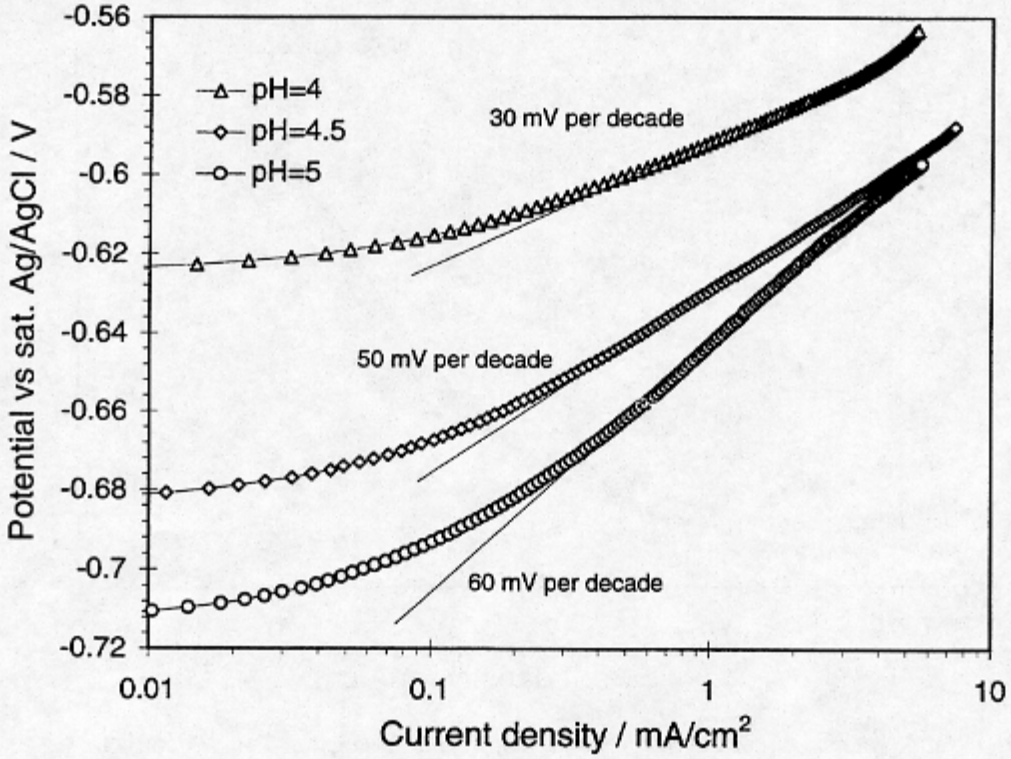

Figure 6 - Potentiodynamic sweeps at intermediate pH and Pco_2 = 1 *bar*, sweep rate : 1 mV/s, $NaClO_4$: 0.2M, 4000 rpm, T=22C, Steel X65.

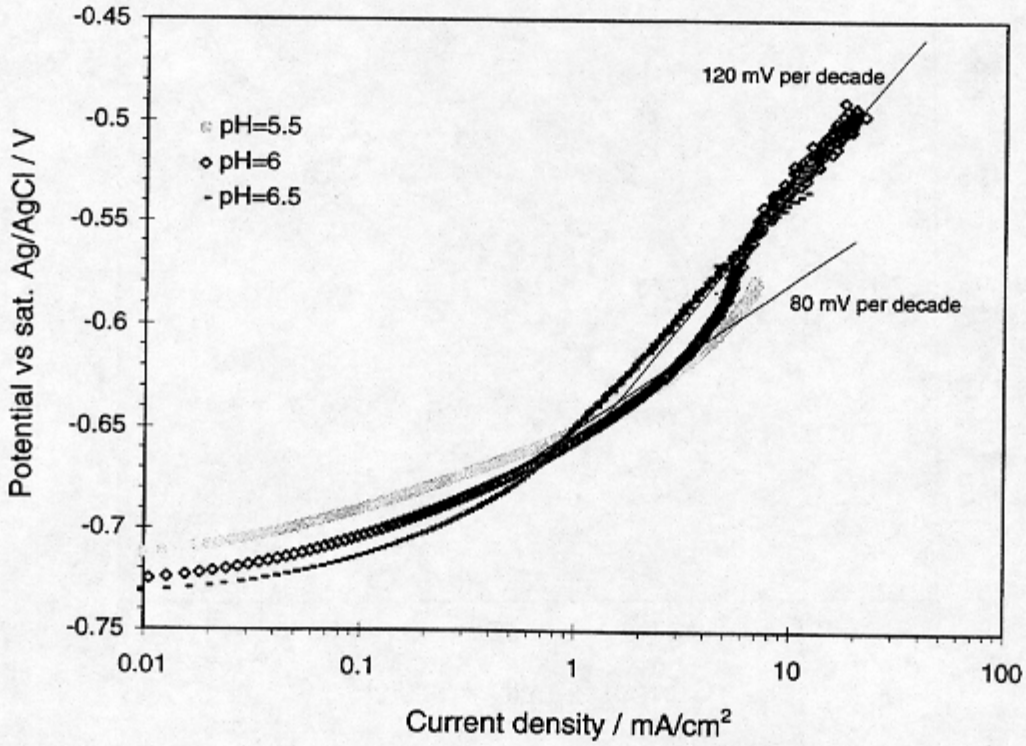

Figure 7 - Potentiodynamic sweeps at high pH and Pco_2 = 0.2 *bar*, sweep rate : 1mV/s, $NaClO_4$: 0.2 M, 4000 rpm, T = 22C, Steel X65.

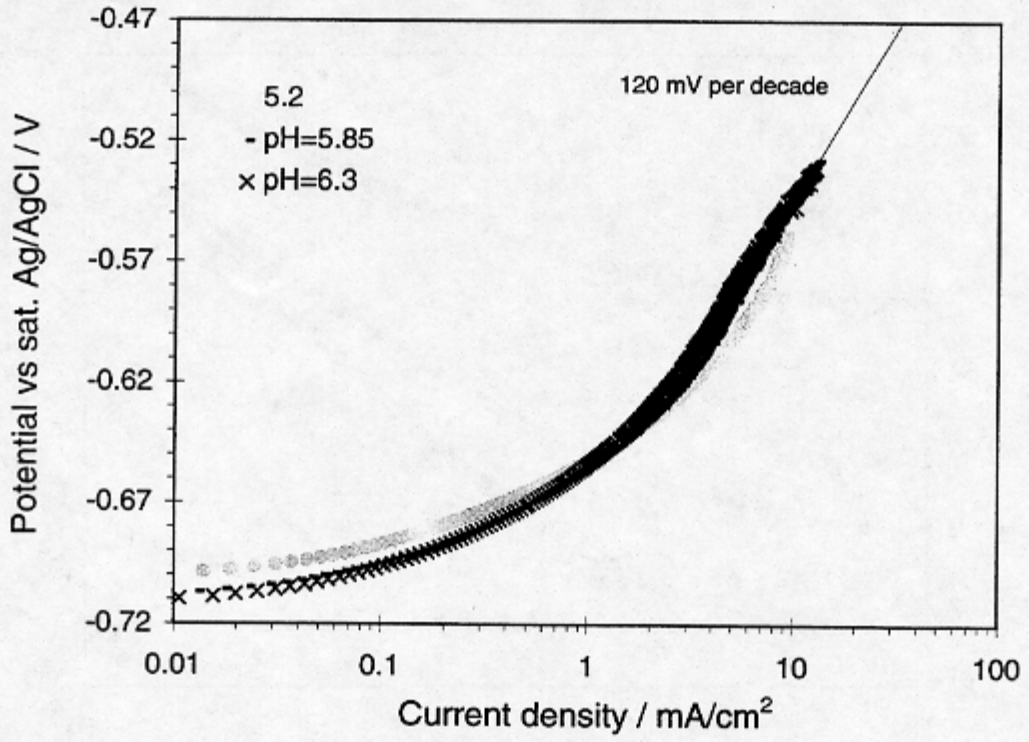

Figure 8 - Potentiodynamic sweeps at high pH and Pco_2 = 1 *bar*, sweep rate : 1mV/s, $NaClO_4$: 0.2 M, 4000 rpm, T = 22C, Steel X65.

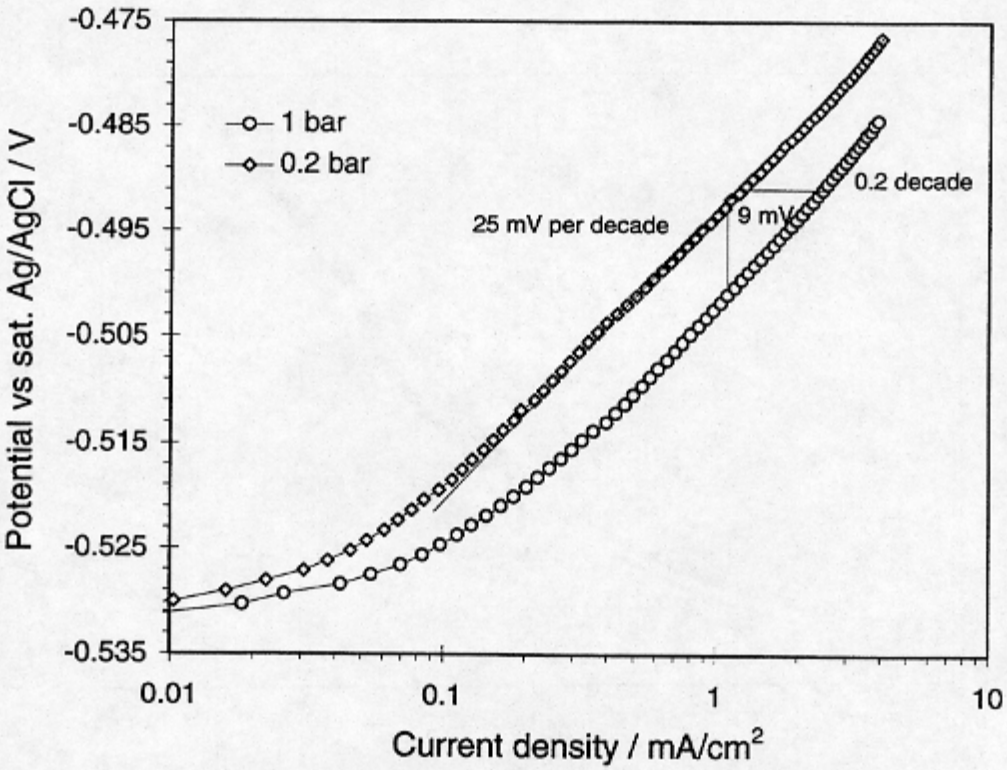

Figure 9 - Potentiodynamic sweeps at pH 2.5, sweep rate : 1 mV/s, NaClO4 : 0.2 M, 4000 rpm, T=22C, Steel X65.

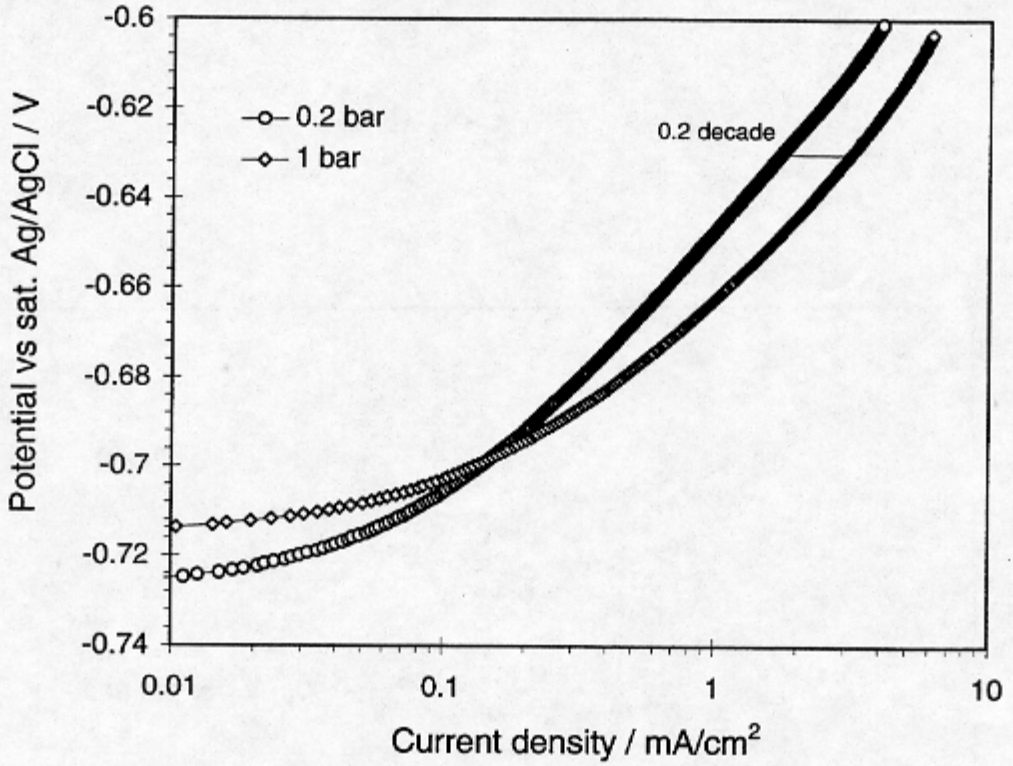

Figure 10 - CO_2 partial pressure effect on potentiodynamic sweeps at pH 6, sweep rate : 1 mV/s, $NaClO_4$: 0.2 M, 4000 rpm, T=22C, Steel X65.

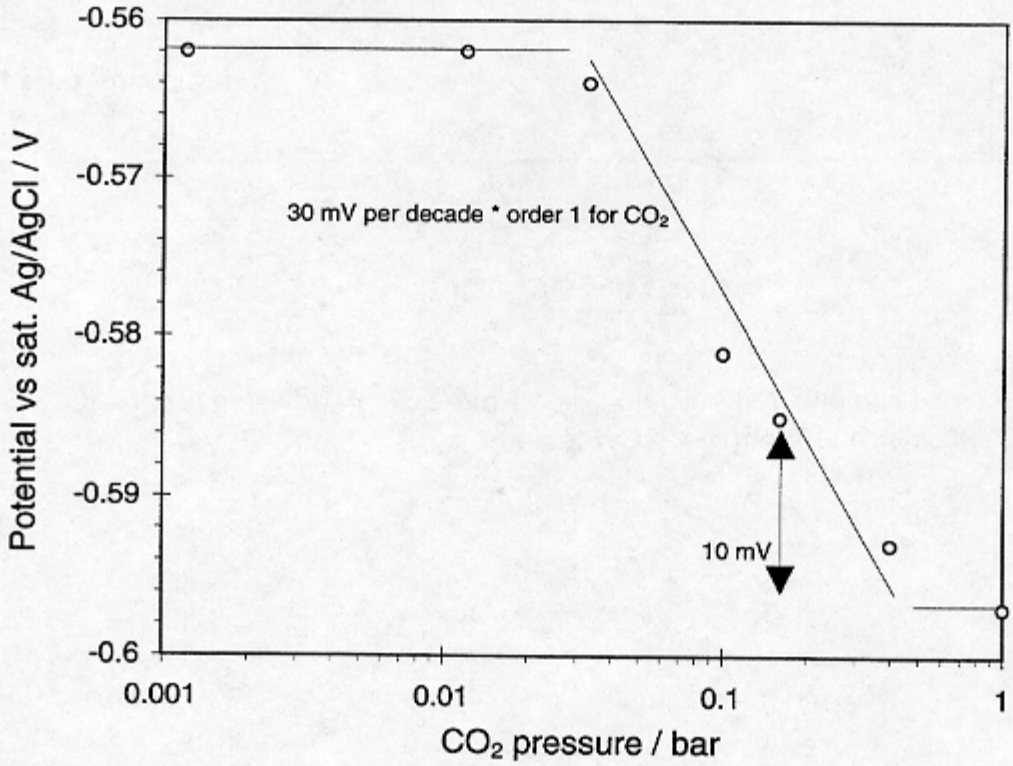

Figure 11 - Galvanostatic measurements at I_{anodic} = 1 mA/cm^2 and pH 3.6, pH adjusted with $HClO_4$ and NaOH, $NaClO_4$: 0.2 M, 4000 rpm, T=22C, Steel X65.

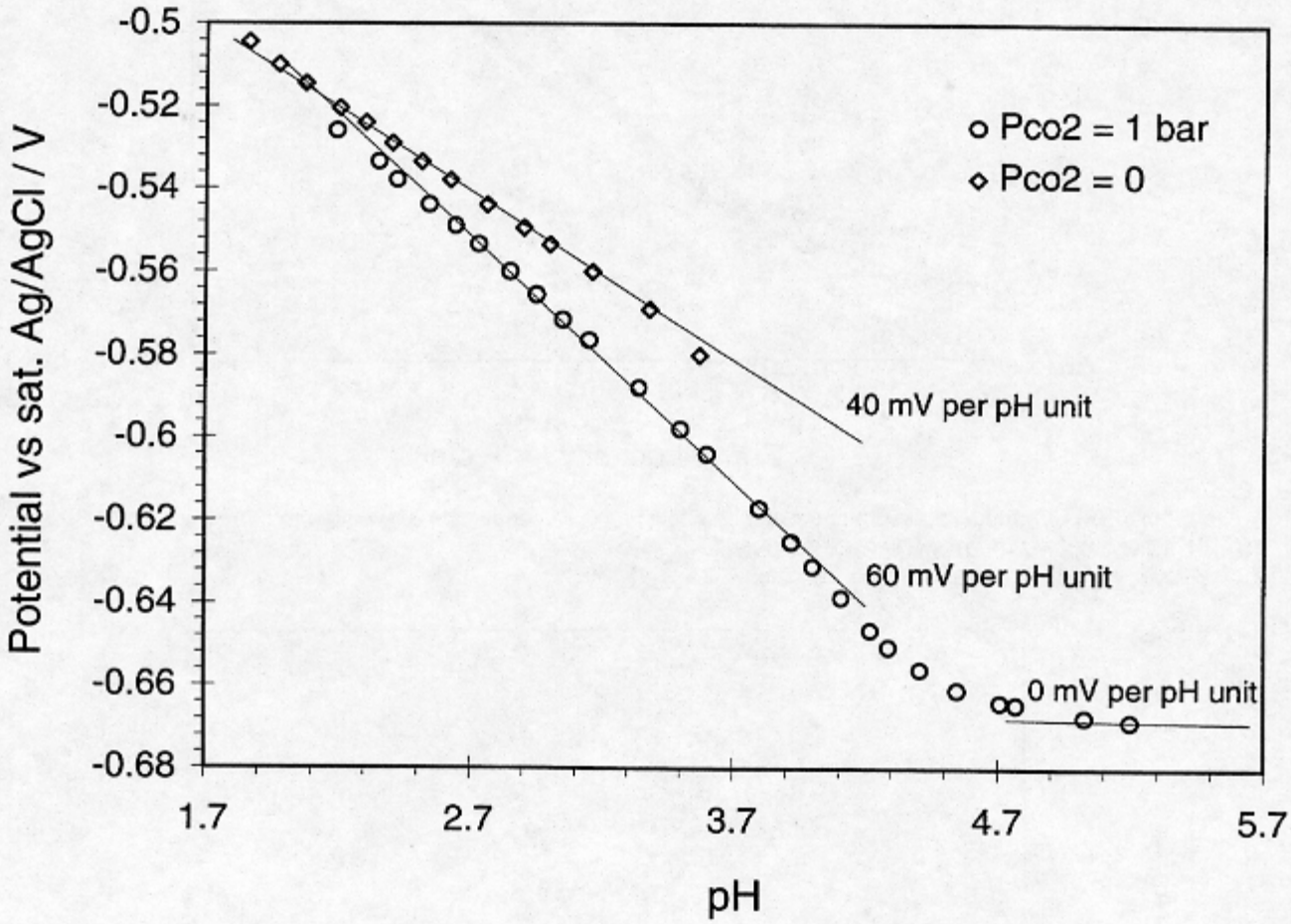

Figure 12 - Galvanostatic measurements at I_{anodic} = 1 mA/cm^2, pH adjusted with $HClO_4$ and $NaHCO_3$, $NaClO_4$: 0.2 M, 4000 *rpm*, T=22C, Steel X65.

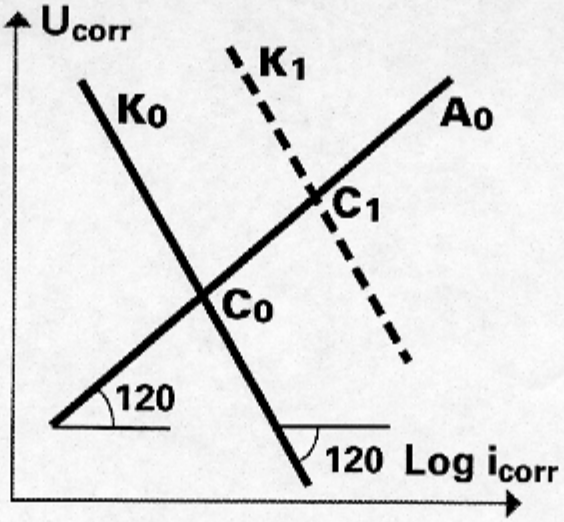

Figure 13 - Evolution of the free corrosion point C when the local pH is higher than 5.

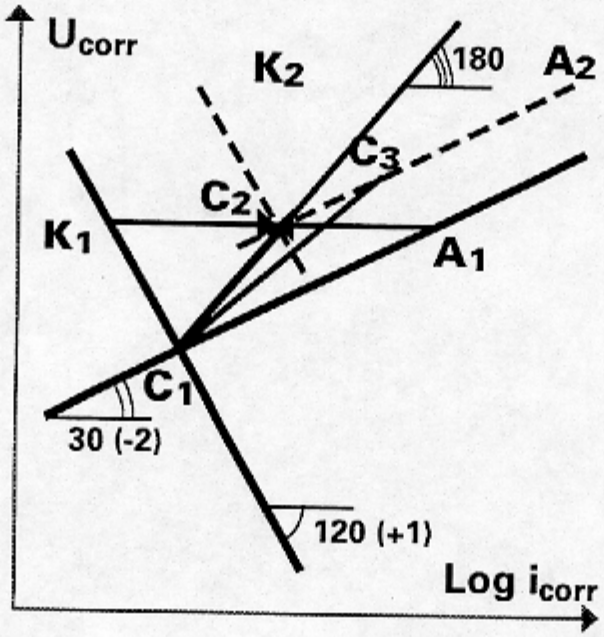

Figure 14 - Evolution of the free corrosion point C when the local pH is lower than 4, due to internal acidizing only (C_1C_2) or to a combination with galvanic coupling (C_1C_3).